

Supporting Information

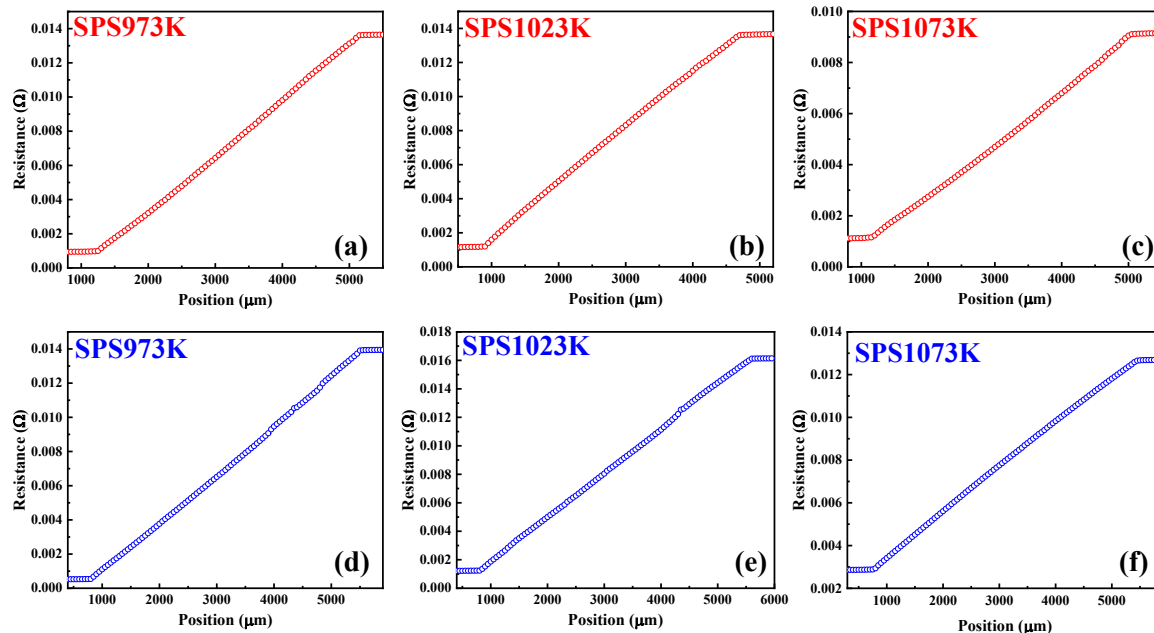


Fig. S1. Resistance scan of powder fabricated $\text{SS}_p/\text{Mg}_3\text{Sb}_{1.5}\text{Bi}_{0.5}/\text{SS}_p$ sintered at (a) 973 K, (b) 1023 K, (c) 1073 K and foil fabricated $\text{SS}_f/\text{Mg}_3\text{Sb}_{1.5}\text{Bi}_{0.5}/\text{SS}_f$ sintered at (d) 973 K, (e) 1023 K, (f) 1073 K.

Table. S1. Specific contact resistivity of $\text{SS}_p/\text{Mg}_3\text{Sb}_{1.5}\text{Bi}_{0.5}/\text{SS}_p$ and $\text{SS}_f/\text{Mg}_3\text{Sb}_{1.5}\text{Bi}_{0.5}/\text{SS}_f$ sintered at 973 K, 1023 K and 1073 K.

Sr. No	Sintering temperature (k)	R_1 (m Ω)	R_2 (m Ω)	ΔR (m Ω)	ρ_c ($\mu\Omega \text{ cm}^2$)
SS p	1.	0.690	0.922	0.232	19.7
	2.	1.322	1.467	0.145	12.3
	3.	1.075	1.167	0.092	7.9
SS f	4.	0.544	0.678	0.134	10.7
	5.	1.240	1.360	0.120	9.7
	6.	1.217	1.400	0.183	8.2

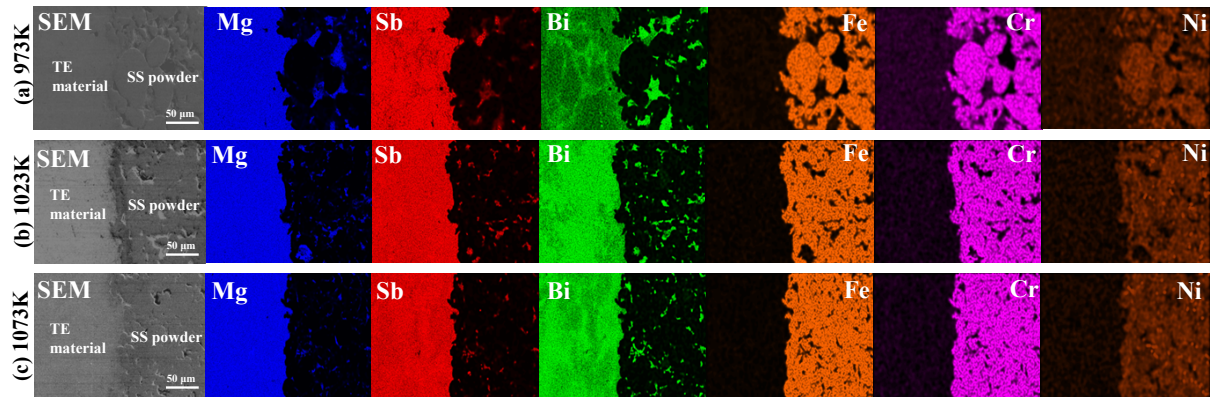


Fig. S2. SEM and EDX of powder fabricated $\text{SS}_p/\text{Mg}_3\text{Sb}_{1.5}\text{Bi}_{0.5}/\text{SS}_p$ sintered at (a) 973 K (b) 1023 K and (c) 1073 K.

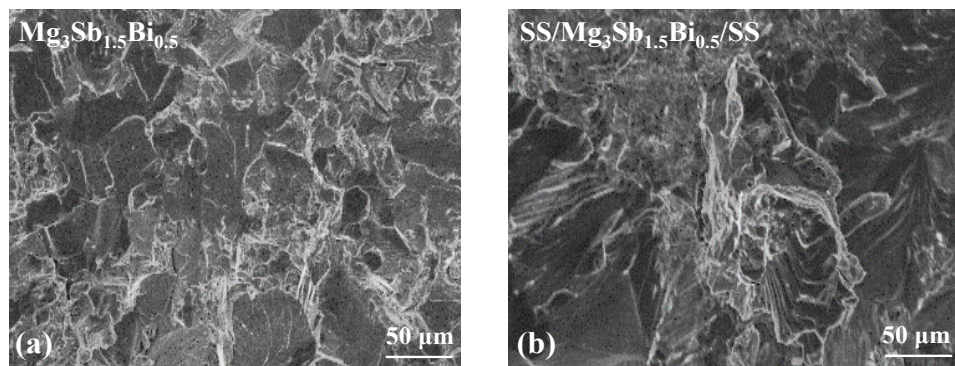


Fig. S3. SEM of $\text{Mg}_3\text{Sb}_{1.5}\text{Bi}_{0.5}$ and $\text{SS}/\text{Mg}_3\text{Sb}_{1.5}\text{Bi}_{0.5}/\text{SS}$ sintered at 1073 K.

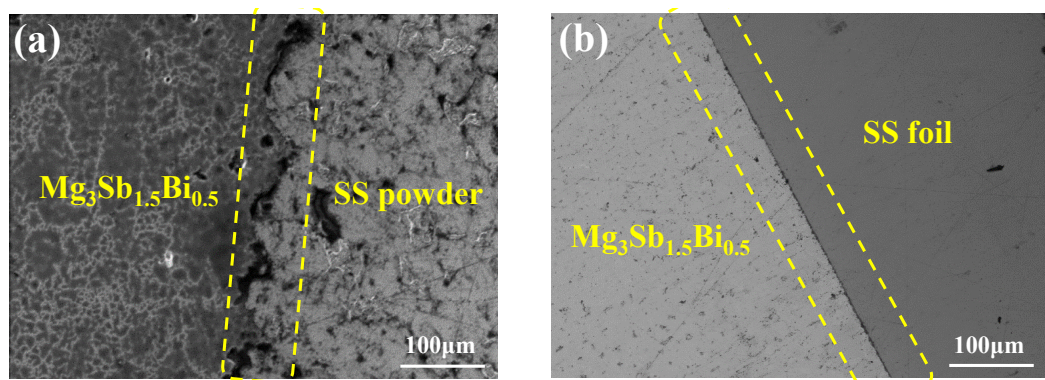


Fig. S4. SEM of (a) $\text{Mg}_3\text{Sb}_{1.5}\text{Bi}_{0.5}/\text{SS}_p$ and (b) $\text{Mg}_3\text{Sb}_{1.5}\text{Bi}_{0.5}/\text{SS}_f$ interfaces sintered at 1073 K.

Fig. S5. EDX and lins scan comparison of stainless steel powder (SS_p) and stainless steel foil (SS_f) fabricated samples at (a) 973 K, (b) 1023 K and (c) 1073 K.

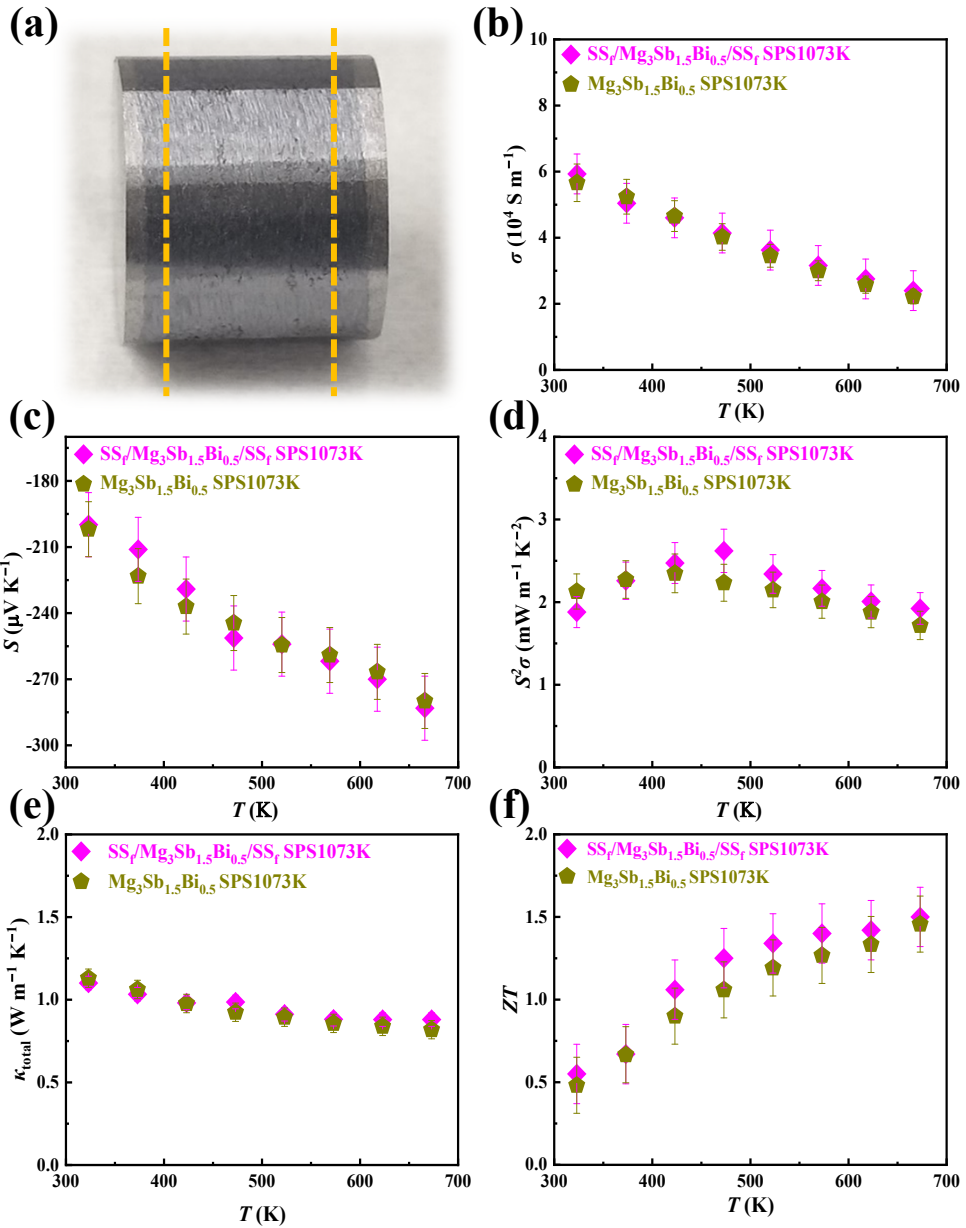


Fig. S6. (a) Image of $\text{SS}_f/\text{Mg}_3\text{Sb}_{1.5}\text{Bi}_{0.5}/\text{SS}_f$ sample. Thermoelectric properties of $\text{SS}_f/\text{Mg}_3\text{Sb}_{1.5}\text{Bi}_{0.5}/\text{SS}_f$ and $\text{Mg}_3\text{Sb}_{1.5}\text{Bi}_{0.5}$ sintered at 1073 K, which includes (b) Electrical conductivity (σ), (c) Seebeck Coefficient (S), (d) Power Factor ($S^2\sigma$), (e) Thermal conductivity (κ_{total}) and (f) ZT .

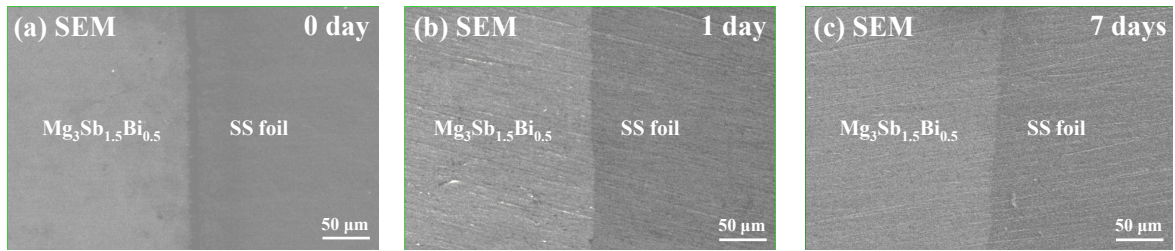


Fig. S7. SEM of foil fabricated Mg₃Sb_{1.5}Bi_{0.5}/SS_f aging at 673K at (a) 0 day, (b) 1 day, and (c) 7 days.

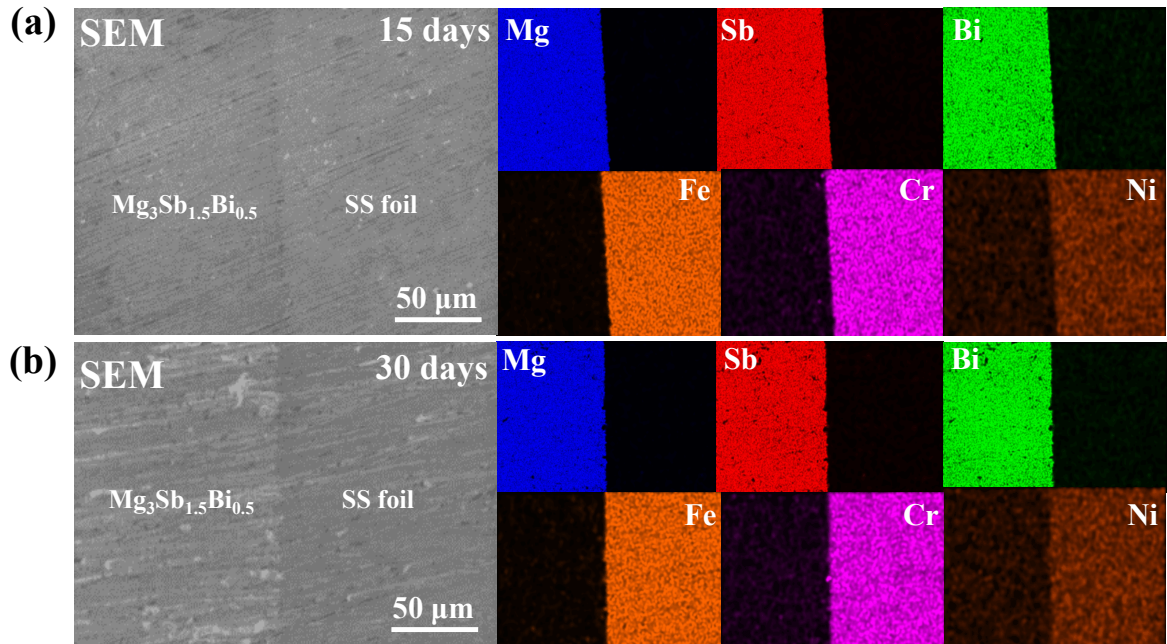


Fig. S8. SEM and EDX of Mg₃Sb_{1.5}Bi_{0.5}/SS_f aging at 673K after (a) 15 days and (b) 30 days.

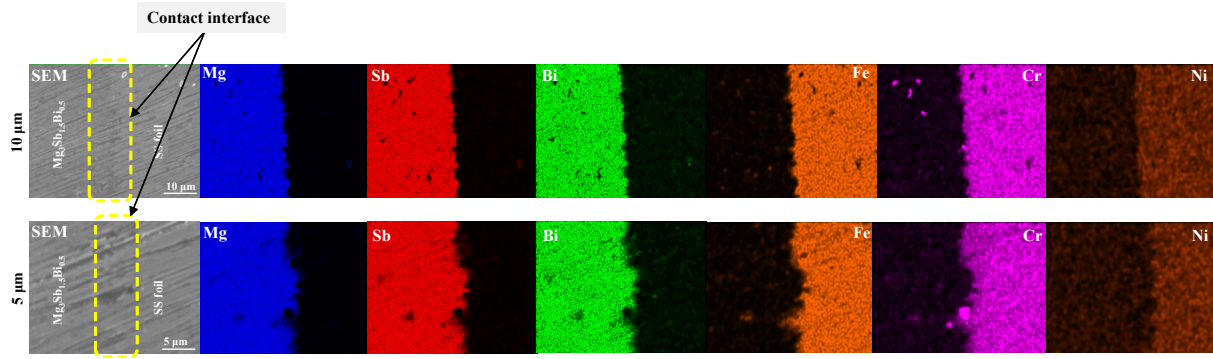


Fig S9. SEM and EDX (10 μm and 5 μm) of $\text{Mg}_3\text{Sb}_{1.5}\text{Bi}_{0.5}/\text{SS}_f$ sintered at 1073 K after aging of 30 days.

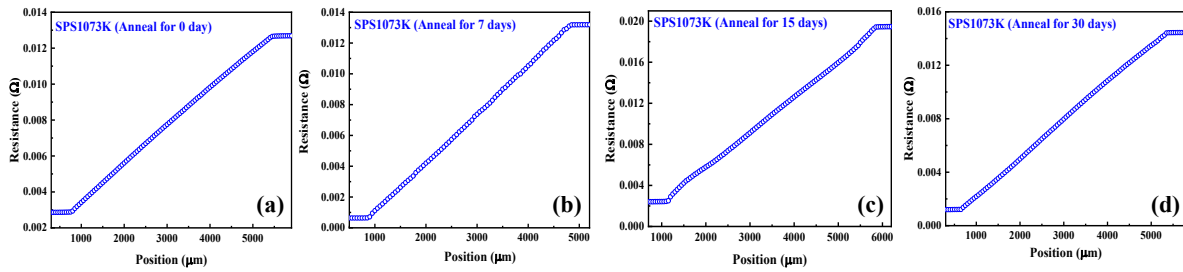


Fig. S10. Resistance scan of $\text{SS}_f/\text{Mg}_3\text{Sb}_{1.5}\text{Bi}_{0.5}/\text{SS}_f$ aging at 673 K at (a) 0 day, (b) 7 days, (c) 15 days and (d) 30 days.

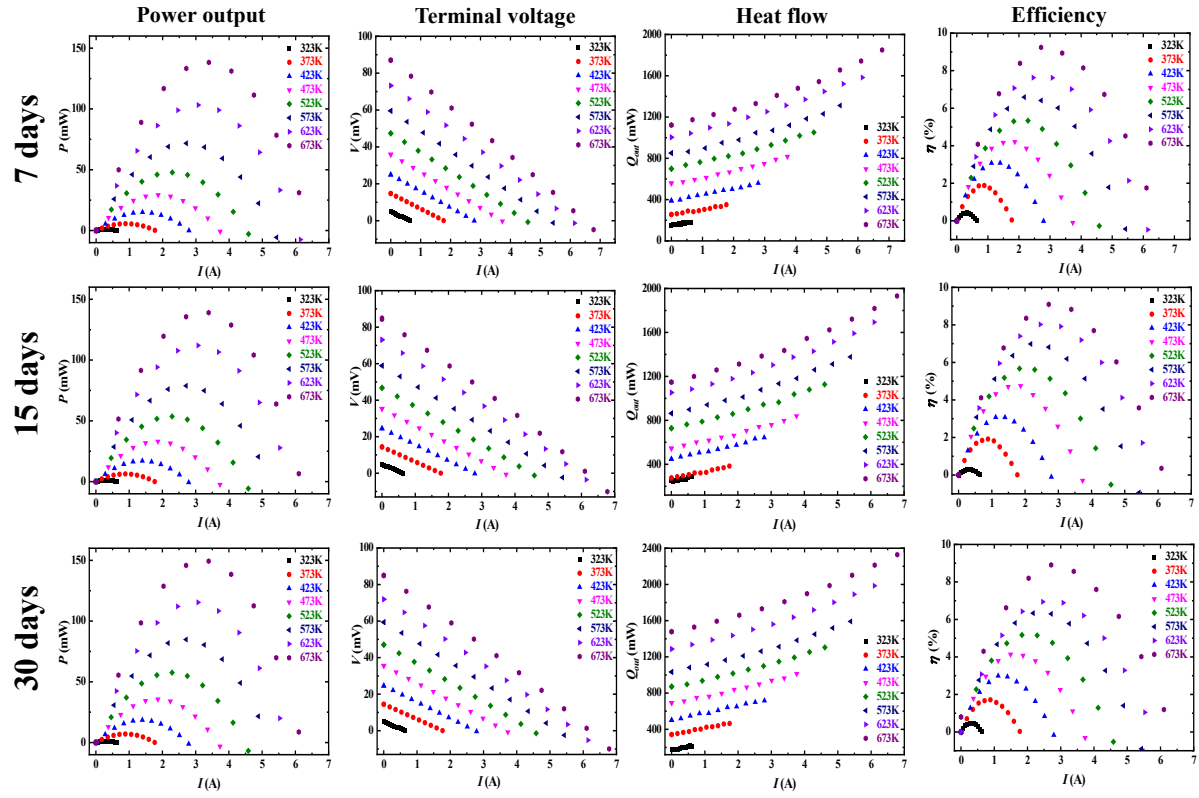


Fig. S11. Power output (P), terminal voltage (V), heat flow (Q_{out}) form cold side and conversion efficiency (η) of $\text{SS}_\text{f}/\text{Mg}_3\text{Sb}_{1.5}\text{Bi}_{0.5}/\text{SS}_\text{f}$ after 7, 15 and 30 days of aging at 673 K.

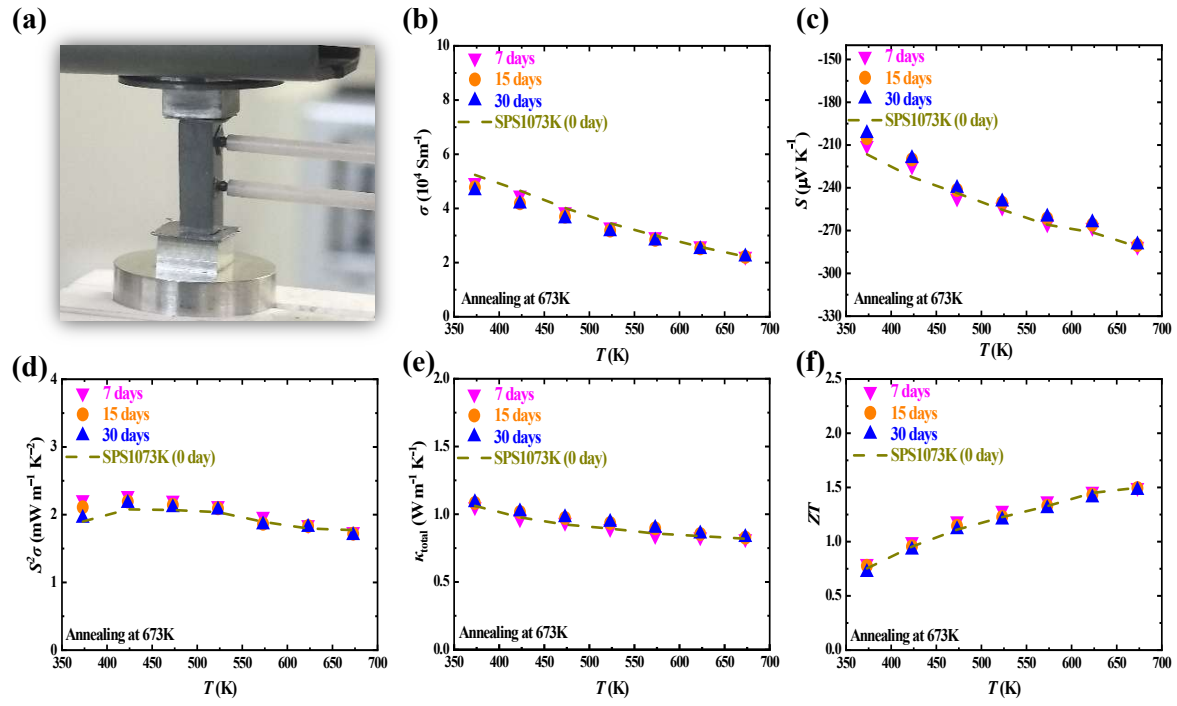


Fig. S12. (a) Four probe (ZEM-3) holders of $\text{Mg}_3\text{Sb}_{1.5}\text{Bi}_{0.5}$ to measure the electrical properties. Thermoelectric (TE) properties of $\text{Mg}_3\text{Sb}_{1.5}\text{Bi}_{0.5}$ aging after 7, 15 and 30 days, including (b) Electrical conductivity (c) Seebeck coefficient (d) Power factor (e) Thermal conductivity and (f) ZT.

Fig. S13. SEM, EDX and Line scan of $Mg_3Sb_{1.5}Bi_{0.5}$ with and without annealing at 673 K after 30days.